Midline serotonergic neurones contribute to widespread synchronized activity in embryonic mouse hindbrain

Peter N. Hunt, Annette K. McCabe and Martha M. Bosma

Department of Biology, University of Washington, Seattle WA 98195-1800, USA

Spontaneous, synchronous activity occurs in motor neurones of the embryonic mouse hindbrain at the stage when rhombomeric segmentation disappears (embryonic day 11.5). The mechanisms generating and synchronizing the activity, however, and the extent to which it is widespread in the hindbrain, are unknown. We show here that spontaneous activity is initiated in the midline of the hindbrain, and propagates laterally to encompass virtually the entire hindbrain synchronously and bilaterally. Separation of the midline region from lateral regions abolishes or slows activity laterally, but not medially. The early differentiating neurones of the midline raphe system are present in the rostral midline and express serotonin at E11.5. Their axons ramify extensively in the marginal zone, cross the midline, and extend at the midline both rostrally into the midbrain and caudally towards the caudal hindbrain. Blockers of serotonin receptors, specifically the 5-HT_{2A} receptor, abolish synchronous activity in the hindbrain, while blockers of other neurotransmitter systems, including GABA and glutamate, do not. In addition, the 5-HT_{2A} receptor is expressed in the marginal regions in the entire medial-to-lateral extent of the hindbrain and in the midline commissural region. Thus, the serotonergic neurones of the developing midline raphe system may play a role in initiating and propagating spontaneous synchronous activity throughout the hindbrain.

(Resubmitted 29 April 2005; accepted after revision 31 May 2005; first published online 2 June 2005)
Corresponding author M. Bosma: Department of Biology, University of Washington, Seattle WA 98195-1800, USA. Email: martibee@u.washington.edu

Spontaneous propagating waves of synchronous electrical activity and their resultant $[Ca^{2+}]_i$ transients are widespread in early brain development (for reviews, see Feller, 1999; Moody & Bosma, 2005). Although spontaneous activity plays important roles in establishing neuronal circuitry and intrinsic cellular properties, the cellular mechanisms that initiate and synchronize it remain obscure. Emergent properties of excitatory networks have been shown to mediate synchronous spontaneous activity in some developing brain regions (Chub & O'Donovan, 1998; Garaschuk *et al.* 1998; O'Donovan, 1999; Menendez de la Prida & Sanchez-Andres, 2000; Tabak *et al.* 2001), while pacemaker regions, identified by surgical and pharmacological pinpointing, have not clearly been shown.

In the chick hindbrain after the period of rhombomeric segmentation, spontaneous firing is synchronized between homologous motor roots on both sides of the hindbrain, and between different motor roots along the rostrocaudal axis (Fortin *et al.* 1995). Our previous experiments used retrograde dextran labelling to identify motor neurones of embryonic mouse hindbrain cranial nerve nuclei and demonstrated that motor neurones develop spontaneous synchronous $[Ca^{2+}]_i$ transients at E11.5 (Gust *et al.* 2003), a time that coincides with the loss of boundaries between rhombomeres (r) 1–7. We observed tight synchronization between motor neurones that were not in close proximity as well as between identified motor neurones and nearby non-labelled neurones. These data imply that a widely distributed mechanism of coordination exists within the hindbrain (Fortin *et al.* 1995), but such a pacemaker region had not been identified.

We demonstrate here that spontaneous synchronized activity at E11.5 in the mouse hindbrain includes large regions of the hindbrain, beyond motor neurone pools. In addition, our results suggest that midline serotonergic neurones participate in driving that activity. Activity propagates from the midline neurones to lateral regions, physical separation of midline neurones from the lateral hindbrain disrupts lateral activity, 5-HT_{2A} receptor antagonists block activity in all regions, and immunoreactive 5-HT_{2A} receptors are present throughout the hindbrain.

 DOI: 10.1113/jphysiol.2005.089581

Methods

Timed-pregnant embryonic day (E) 11.5 Swiss/Webster mice (E0.5 defined as the morning of plug formation) were killed by an excess of CO_2 in accordance with the regulations of the University of Washington Animal Care Committee (IACUC). Embryos were removed from uteri into carbogen (95% O_2–5% CO_2)-bubbled ACSF, containing (mM): 119 NaCl, 2.5 KCl, 1.3 $MgCl_2$, 2.5 $CaCl_2$, 1.0 NaH_2PO_4, 26.2 $NaHCO_3$, 11 glucose. Embryos were unilaterally injected with Texas Red-conjugated dextran (relative molecular mass 3000, Molecular Probes, Eugene, OR, USA) into the mandibular arch and branchial arches 1–2 (Gust *et al.* 2003), and the dye allowed to transport for 1–8 h at 23°C. For most intracellular Ca^{2+} ($[Ca^{2+}]_i$) imaging experiments, the hindbrains were dissected from the surrounding tissue and the dorsal midline was cut; tissue was folded back, so that dorsal regions were lateral to the ventral midline during recording (Gust *et al.* 2003). For some experiments using horizontal slices of hindbrain (see Fig. 8), whole embryos were embedded in low-temperature agarose (Sigma, USA), immersed in ice-cold carbogen-bubbled ACSF, and sliced at 200 μm on a vibratome. Slices were allowed to recover at room temperature before use. Whole hindbrains or slices were loaded with 1.75 μM fluo-4 AM plus 0.07% Pluronic F127 (Molecular Probes) for 15 min. After rinsing, the hindbrain was laid in the chamber of an inverted microscope with the marginal zone down. All experiments were performed at approximately 23°C. Tissue was perfused with carbogen-bubbled ACSF, and $[Ca^{2+}]_i$ signals were obtained from images of the fluo-4 signal, monitored with 488 nm excitation wavelength, taken every 0.4–3 s. The dextran signal was visualized using 594 nm excitation. Images were recorded with a cooled CCD camera (Princeton Instruments, Trenton, NJ, USA), and the $[Ca^{2+}]_i$ signals were sampled during the experiment using the software package MetaFluor (Universal Imaging, West Chester, PA, USA). Each $[Ca^{2+}]_i$ value is the average intensity of the pixels within defined regions shown in the figures; the regions included 5–15 cells. Pharmacological agents (Ketanserin and methiothepin from Tocris Bioscience, Ellisville, MO, USA; all others from Sigma, St Louis, MO, USA) in solution were bubbled with carbogen and were delivered through a separate port, and final values of modulation were determined after activity stabilized at the new value. Ketanserin was applied for 22 ± 2 min ($n = 24$), spiperone was applied for 20 ± 3 min ($n = 7$), and DOI was applied for 18 ± 1 min ($n = 31$). Data were evaluated by assessing individual records for $[Ca^{2+}]_i$ transients; each transient was scored as a positive event if it crossed a threshold value of 10% of the value of the largest event in the record. Traces in Figs 2, 3, 6 and 8 are stacked vertically in order to present individual traces more clearly; those in Fig. 6 were smoothed to remove a slow decline due to photobleaching. With these exceptions, $[Ca^{2+}]_i$ records were not manipulated in any other way. All results are expressed as means ± S.E.M., and significance determined by use of Student's *t* test.

Immunocytochemistry for the neuronal marker TuJ1, serotonin and the 5-HT_{2A} receptor was performed after whole embryo fixation in 4°C freshly made 4% paraformaldehyde in phosphate buffered saline (PBS) containing (mM): 3.16 NaH_2PO_4, 6.84 Na_2HPO_4, 150 NaCl, pH 7.2. Embryos were immersed in 20% sucrose in PBS overnight, embedded and frozen in OCT medium, and sliced at 20 μm in a cryostat at −20°C; sections from both sagittal and horizontal planes were examined. Tissue was blocked for 1 h with 10% normal goat serum (Jackson ImmunoResearch Laboratories, West Grove, PA, USA), and incubated for 48–72 h at 4°C with 1 : 1000 polyclonal anti-TuJ1 antibody (Babco, Berkeley, CA, USA), 1 : 3000 antiserotonin polyclonal antibody (ImmunoStar, Hudson, WI, USA), or 1 : 500 anti5-HT_{2A} monoclonal antibody (BD PharMingen, Chemicon, San Diego, CA, USA). Secondary antibody was either Alexa 488- or Alexa 594-conjugated goat-antirabbit or antimouse (Molecular Probes) and was applied at 1 : 200 for 1 h at room temperature. In some experiments, the fluorescent DNA marker 4′,6′-diamidino-2-phenylindole hydrochloride (DAPI) was applied at 1 : 1000 in PBS for 10 min. Slices were examined in a Bio-Rad confocal (Bio-Rad, Hercules, CA, USA) and images manipulated with Adobe Photoshop (Adobe Systems, San Jose, CA, USA).

Counting of neuronal cells to identify the proportion of serotonergic neurones was performed by examining the rostral–caudal extent of the hindbrain where serotonergic neurones are observed (approximately 680 μm, see Fig. 4*B*). This area was sampled by taking every third slice in a rostral–caudal sequence and counting cell profiles in the central optical plane (3 μm thick) only. Any DAPI profile less than one half-diameter of the average of the neurones around it was not included in the cell counts. As neurones become postmitotic and exit the cell cycle, they move towards the pial side of the ventricular zone and begin to express neuronal characteristics such as TuJ1 and serotonin, but often have processes that trail towards the ventricular zone. These neurones that were newly postmitotic were included in the neuronal counts. The most rostral section of the serotonergic neurone nucleus was not included in the total neurone count. However, even at that rostral border, 59% of the TuJ1-positive neurones ($n = 114$ neurones) were immunopositive for serotonin.

Results

We first asked how widespread spontaneous activity is in the hindbrain, and over how large an area it is synchronized. To provide anatomical landmarks for these

experiments, which were done in the open hindbrain rather than slice preparations, we injected the mandibular arch and branchial arches 1 and 2 unilaterally with Texas Red-conjugated dextran to identify motor neurones and their axonal projections. An example of these axonal patterns is shown in Fig. 1*A*, a montage of eight individual fields which are digitally overlapped to include the majority of the left side of a hindbrain. The midline is indicated at the right by the long vertical line, and the former rhombomere borders indicated. More laterally, the labelled trigeminal (nV) motor neurones in former r2–3 are seen, near their lateral exit point (EP-V, *). Facial (nVII) motor neurones are found medially in former r5–6 and in the facial axons coursing towards their lateral exit point in former r4 (EP-VII, *). These anatomical features are shown schematically in Fig. 1*B*.

The hindbrain was then imaged for spontaneous $[Ca^{2+}]_i$ transients by recording changes in fluorescence in an array of small recording sites within 448 μm × 350 μm rectangular fields (the image size of our 20× objective) of identified hindbrain areas; the rectangular field was then positioned over a different part of the same hindbrain until activity in the entire left side was sequentially mapped. An example of one such sequentially sampled field, with three of the individual imaged sites within that array, is indicated by the outlined rectangular area in Fig. 1*A*; all eight fields for this experiment are indicated schematically in Fig. 1*B*. The field observed at 488 nm wavelength illumination to evaluate Ca^{2+} signals from of the fluo-4 indicator dye is shown in Fig. 1*C*. The midline region typically contains a large number of well-loaded cell bodies, and the fan of the nVII axons can be seen. The focal plane for these experiments was in the marginal zone, which contains many fibres but relatively few cell bodies. A similar field is shown in Fig. 1*D*, demonstrating the extensive axonal processes (see also Fig. 8 for another example of fluo-4 loading.) The fluo-4 loading of dextran-identified motor neurones is shown in colour in Fig. 5*A*.

$[Ca^{2+}]_i$ records from three individual imaged sites within each of the eight sampling fields are shown next to each field in Fig. 1*A*. Spontaneous activity was detected in all fields imaged, indicating that spontaneous activity occurs over large portions of the hindbrain, extending on the rostro-caudal axis from the former r2 through r6, and from the midline past the lateral exit points of the branchiomeric motor neurones. Within each field, $[Ca^{2+}]_i$ transients in all recording sites were synchronized, showing that activity is synchronized over at least the entire 448 μm × 350 μm of a single field. Experiments at lower magnification (see below) show that synchronicity extends over areas at least 895 μm × 700 μm (n = 19), encompassing approximately one-third of the total area of the half-hindbrain, including almost the entire mediolateral dimension and at least two former rhombomeres in the anterior–posterior dimension. Experiments in which regions lateral to the midline on both sides of the hindbrain were sampled simultaneously demonstrated that the two sides of the hindbrain are synchronously active (n = 30, see also Fig. 8). Thus, large regions of the hindbrain and most likely the entire hindbrain bilaterally express spontaneous synchronized activity.

Such widespread spontaneous activity might be generated as an emergent property of the neural circuitry at these stages, or might be driven by a discrete pacemaker region. In the above experiments, we observed that some transients (27 ± 6%, n = 19 experiments) occurred only near the midline and were not recorded laterally; isolated lateral transients were never observed. Several examples of midline-only transients are marked with open circles in Figs 1*A*, 2*A* and 3*A*.

To determine whether the occurrence of midline-only transients indicates a pacemaker function for some population of midline neurones, we characterized three properties of midline neurones. First, whether the occurrence of midline-only transients was consistent enough to be reflected in a higher mean frequency of activity in midline neurones. Second, whether global transients consistently propagated from the midline neurones to lateral regions. Third, whether physical separation of midline and lateral hindbrain regions disrupted lateral activity while leaving midline activity intact. In these experiments we defined the midline region as the obvious band of brightly fluo-4-loaded cells delimited laterally by a soma-sparse region containing mainly nerve fibres and cranial motor nuclei (Fig. 1*C*). This band of cell bodies extended 63 ± 6 μm (n = 10) bilaterally of the anatomical midline. Within this defined region, the frequency of activity was 3.0 ± 0.3 events min^{-1}, while that in lateral regions was 2.1 ± 0.4 events min^{-1} (n = 18, P = 0.013). These data suggest that the midline serves as an initiator for synchronous activity in the hindbrain and that propagation to the lateral 'follower' regions occurs in approximately 70% of midline events.

To measure the direction and speed of propagation of $[Ca^{2+}]_i$ transients we used an array of 9–12 equally spaced small recording sites, beginning approximately 25 μm from the anatomical midline (within the bright band of fluo-4-loaded cells) and spanning between 600 and 700 μm of the mediolateral axis. Using this recording array, activity was observed that propagated from the midline towards more lateral regions at a rate of 241 ± 18 μm s^{-1} (Fig. 2, n = 11 measurements in 8 preparations). Propagation of widespread events from lateral to medial regions was not observed.

If midline activity initiates activity in lateral regions, physical separation of lateral and medial regions should inhibit lateral activity, or desynchronize it from the midline. To test this, activity was imaged in the intact

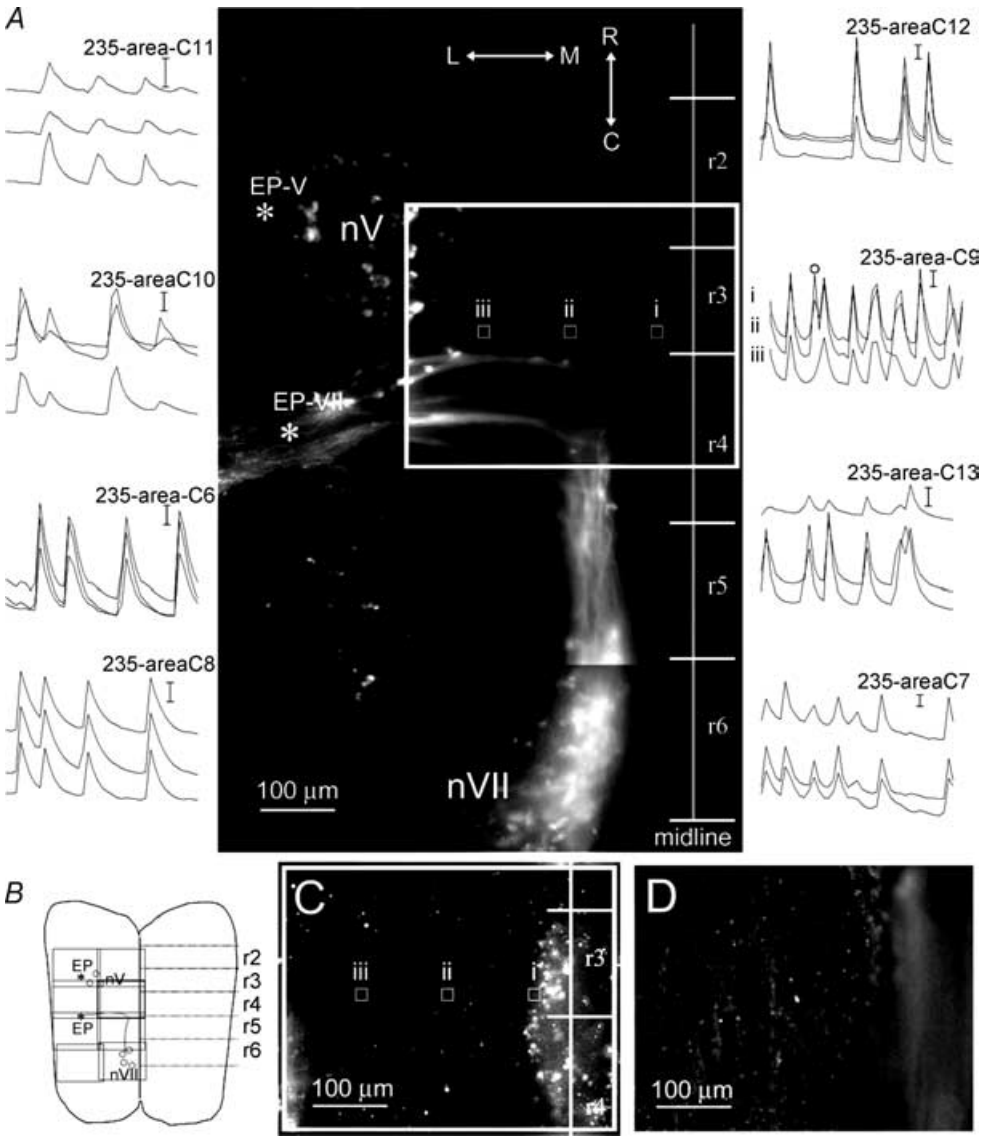

Figure 1. A sequential series of $[Ca^{2+}]_i$ imaging experiments in identified regions of one half of a hindbrain shows that synchronization of $[Ca^{2+}]_i$ signals is found in each region of the hindbrain

A, the central portion of the figure shows anatomical landmarks identified by dextran labelling of branchiomeric motor neurones, taken at a wavelength of 594 nm. The midline is indicated by the vertical line to the right; positions of the former rhombomere borders are indicated with horizontal bars on the midline; arrows at top of figure indicate the rostral–caudal and medial–lateral axes of the tissue. Trigeminal motor neurones are seen in the upper left of the montage (nV) near their axonal exit point (EP-V, *); somata for the facial motor neurones (nVII) are near the midline with their axons fanning laterally toward the VII exit point (EP-VII, *). The outlined rectangle shows one of the eight imaging fields in this experiment. Three small squares (i, ii, iii) are example sites yielding the resultant $[Ca^{2+}]_i$ traces in the plot immediately to the right of this field within the montage, and are a portion of the recordings resulting from the larger array that covers the entire field (other sites of the array not shown). Insets: $[Ca^{2+}]_i$ signals were recorded from overlapping fields, and examples of activity in each field displayed in the adjacent inset as a 2-min segment of activity obtained from recording sites arrayed on the rectangular field. Vertical scale bars indicate 1 unit of change in fluorescence. *B*, schematic diagram depicting the montage of the fields of the hindbrain in part *A*, and the anatomical landmarks illustrated by retrograde dextran labelling. *C*, the same rectangular field outlined in part *A*, taken at 488 nm to show the fluo-4 loading of the tissue. Cells at the midline are individually loaded, and the axons from the nVII fan can be seen. *D*, image from a different experiment on the field of the r5-midline area, taken at 488 nm to show the axon fibres in the marginal zone of the hindbrain.

hindbrain; medial and lateral regions were then completely cut apart and the tissue re-imaged as two separate portions (Fig. 3). In 16/18 experiments, the activity of transients in lateral tissue stopped entirely ($n = 6$) or the frequency decreased ($n = 10$; from 2.1 ± 0.4 to 0.7 ± 0.2 events min^{-1}, $P < 0.001$) after separation. In the remaining two experiments, the initial lateral activity was relatively slow (0.4 and 0.38 events min^{-1}), and the activity after separation from the midline increased in each case to 0.6 events min^{-1}. In contrast, the frequency of activity in midline tissue was not affected (from 3.0 ± 0.3 to 2.6 ± 0.3 events min^{-1}, $P = 0.3$, $n = 18$) (Fig. 3*D*). When activity remained in isolated lateral regions, it was no longer synchronous with that in medial tissue (compare Fig. 3*A* and *B*).

These experiments suggest that in intact hindbrain, medial cells in a region within approximately 125 μm of the midline serve as drivers for overall activity in both medial and lateral regions. This also demonstrates that lateral tissue, in some preparations, is able to generate spontaneous activity at a frequency that is overridden in intact hindbrain by the midline driver.

The serotonergic raphe neurones are among the most prominent midline neurones in the embryonic hindbrain. This system develops as two groups of neurones within the hindbrain – a rostral group that begins to express serotonin at E11.25–11.5 in mouse, and a caudal group that expresses serotonin one day later (Hendricks *et al.* 2003). To determine whether these serotonergic neurones are located at the same points that defined our midline neurones in the above imaging experiments, we performed immunocytochemistry for serotonin (Fig. 4). In a sagittal section taken approximately 20 μm lateral to the midline, serotonin-immunoreactive somata are observed; in addition, immunopositive axons can be seen extending both rostrally into the midbrain and caudally towards the spinal cord (Fig. 4*A*). In a section taken approximately 60 μm lateral to the midline in the sagittal plane, a larger group of serotonin-immunoreactive somata are observed; this indicates that the somata are located at least within 20 μm of the midline, and extend laterally at least 60–80 μm. In the anterior–posterior axis, serotonin-immunopositive somata are aggregated in a group beginning 150 μm caudal of the isthmus and extending approximately 680 μm caudally into the hindbrain (Fig. 4*B*). When examined in horizontal sections (Fig. 4*C*), serotonin-immunoreactive neurones are located immediately ventral to the ventricular zone, in a group ending approximately 150 μm from the midline (the non-neuronal cells of the floor plate are medial to the serotonergic cell bodies). These neurones have extensive processes in the axon-dense marginal zone, including some that cross the midline (Fig. 4*C*). Thus the serotonergic neurones are in the same region as the band of fluo-4 loaded cell bodies that defined the midline region in the imaging experiments above, and within which spontaneous activity appears to originate.

In order for these serotonergic midline neurones to play a role in initiation of spontaneous activity, 5-HT

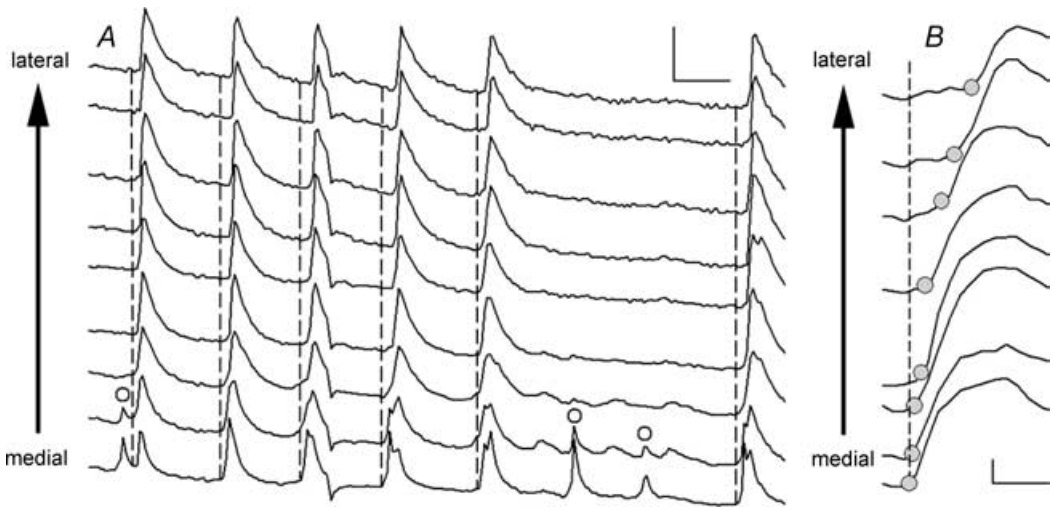

Figure 2. Propagation of $[Ca^{2+}]_i$ signals from midline to lateral regions in the 'open hindbrain' preparation
Both sets of traces are taken from experiments where a field of approximately 895 μm × 700 μm was sampled with an array of recording sites. *A*, records from medial to lateral regions were stacked vertically to show the wave of activity propagating away from the midline (midline at bottom; region at top is 478 μm lateral to that at bottom). Events that did not propagate from the midline are indicated by open circles. Scale bars are 1 unit of change in fluorescence and 20 s. *B*, expanded records sampled at 0.4 s from a different experiment. Grey dots are at the initial upstroke of $[Ca^{2+}]_i$ transients taken from regions separated by 662 μm. Scale bars are 2 units of change in fluorescence and 2 s.

receptors must be present in the hindbrain at this stage. To determine this, we performed immunocytochemistry for the 5-HT_{2A} receptor. Figure 5*B*, a horizontal cryosection from an E11.5 b1-dextran-injected animal, demonstrates localization of the 5-HT_{2A} receptor. The receptor is expressed in decussating axons at the midline and in the entire marginal zone of the hindbrain, from medially near the serotonergic neurone region, laterally past the exit points of the branchiomeric motor axons. Label is reduced in the region of the trigeminal motor nucleus (nV), where the dextran-identified motor neurones fluorescing at 594 nm (red) are shown. Expression of the 5-HT_{2A} receptor is also seen on the motor axons exiting the hindbrain, and the sensory axons of the trigeminal sensory ganglion (gV) outside of the hindbrain.

Localization of the 5-HT_{2A} receptor was compared to the position of serotonergic neurones in the midline region in tissue on which dual immunocytochemistry was performed (Fig. 5*C*). Receptor expression is high in the axons crossing the ventral midline commissure. Receptor expression is also high in a few serotonin-immunoreactive neurones (arrowheads). Outside of the high expression in the serotonin neurone area and in the medio-lateral extent of the marginal zone, 5-HT_{2A} receptor expression is punctate in the cell body layer (future grey matter), and does not extend into the ventricular zone.

If serotonergic neurones of the midline contribute to initiating widespread spontaneous activity, serotonin receptor antagonists should block activity or modulate lateral spread. Ketanserin (an antagonist at the 5-HT_{2A}

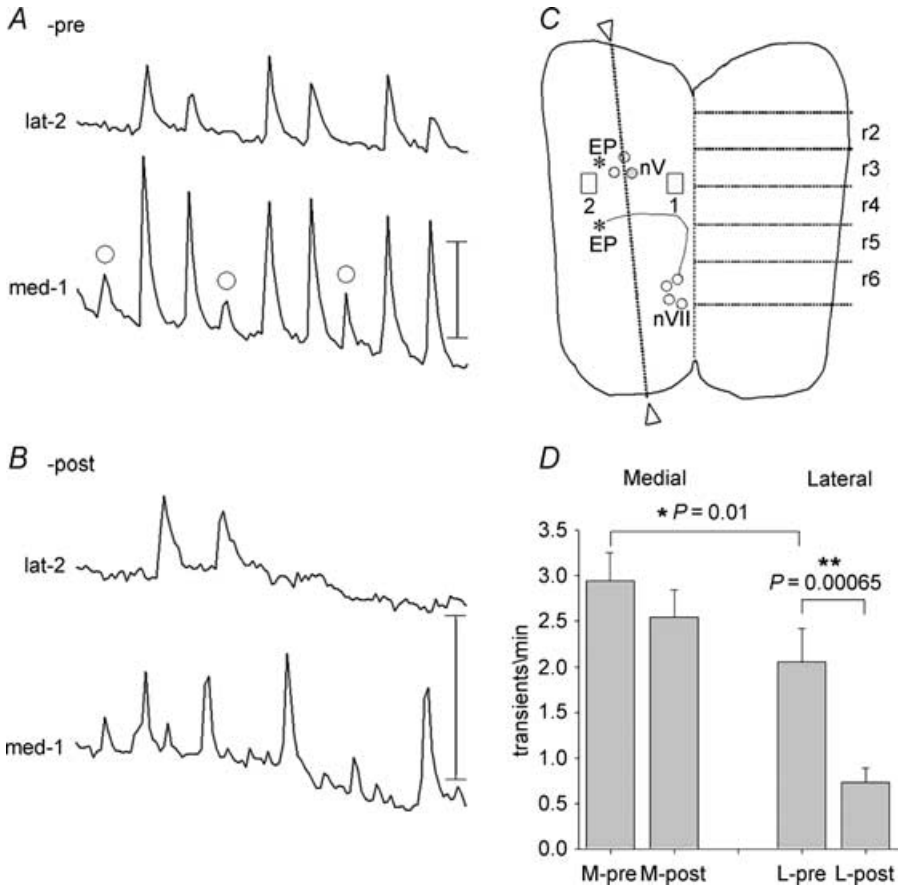

Figure 3. Midline tissue drives laterally propagating activity
A, $[Ca^{2+}]_i$ transients in 4-min segments of recording from medial (lower record, from site 1) and lateral (upper record, from site 2) areas from an intact hindbrain. Recording regions are shown as grey boxes in the drawing in part *C*, with site 1 being the medial recording position, site 2 being the lateral recording position. Open circles mark events that did not propagate into the lateral tissue. Scale bars are 1 unit of change in fluorescence for both *A* and *B*. *B*, same regions after complete vertical transection of the hindbrain at the dashed line shown in part *C*. *C*, drawing of hindbrain indicating the recording configuration and the relative position of the cut through the tissue. *D*, bar graph showing collated results of separation experiments (n =18); the frequency of lateral events is lower initially (M-pre compared to L-pre, $^*P = 0.01$), and decreases significantly after connections from the medial regions are cut (L-pre compared to L-post, $^{**}P = 0.00065$). Frequency of medial regions is unaffected by separation from lateral tissues (M-pre compared to M-post, $P = 0.3$).

receptor; Barnes & Sharp, 1999) had no effect on spontaneous activity at a concentration of 1 μM (Fig. 6*A*, $n = 3$); at 5 μM, the activity slowed to 76 ± 3% of control (6/7 experiments), or was abolished (1/7 experiments). When 10 μM ketanserin was applied, it either slowed the activity (to 43 ± 1% of control, 4/26 cases) or abolished activity completely (22/26 cases) in a reversible manner (Fig. 6*B*). In three cases, there was a slight facilitation of the response to 10 μM ketanserin (increase in frequency to 108%); no facilitation was seen at lower doses. Application of spiperone, another 5-HT_{2A} receptor blocker, had no effect at 10 nM (Fig. 6*C*, $n = 3$), but at 20 nM completely and reversibly blocked the activity (Fig. 6*D*, $n = 6$). Although activity did return with drug washoff, it was small compared to the control condition. This is in part due to the fact that the amplitude of $[Ca^{2+}]_i$ transients tended to diminish over the course of these long experiments (see Fig. 6*A* and *C*). However, recovery included synchronous transients between regions, indicating that block of the 5-HT_{2A} receptor did not de-synchronize events between cells, but appeared to block the initiation of synchronized spontaneous activity. Methiothepin, a 5-$HT_{1B/1D/2C/7}$ antagonist, at 100 μM, did not block activity ($n = 4$). With prolonged application of ketanserin (45–60 min), activity remained blocked, suggesting that other transmitters do not assume the role of initiating synchronization in the hindbrain. This is unlike the situation in spinal cord, where multiple transmitters involved in network synchronization are able to re-initiate activity when one transmitter is blocked (O'Donovan, 1999). Blockade of receptors for glutamate (CNQX – 25 μM, MK801 – 20 μM), glycine (strychnine – 5 μM), GABA (bicuculline – 50 μM, picrotoxin – 10 μM), ACh (d-tubocurarine – 10 μM), or noradrenaline (yohimbine – 25–50 nM, prazosin – 25–50 nM) alone or in combination, did not block activity (data not shown). These data demonstrate that serotonin is unique in its ability to mediate spontaneous activity, and further implicates the midline serotonergic neurones as the primary initiators of that activity.

Serotonin, either alone or after inhibition of the serotonin transporter with citalopram (5 nM, $n = 8$), at concentrations of 1.0 μM ($n = 2$) or at 10–50 μM ($n = 16$) did not modulate the activity. DOI (a 5-HT_{2A} receptor specific agonist) at a concentration of 5 μM increased the frequency of activity in 1/7 experiments; there was no effect in the remaining experiments. At 20–50 μM, DOI elicited an increase in midline or lateral activity in approximately half (10/23) of the preparations (1.9 ± 0.2-fold increase, $n = 8$; DOI also initiated activity in two quiescent preparations), while having no effect in 13/23 preparations; however, these effects were not significant when the entire sample was considered. The variability of the DOI response and the lack of any significant effect of serotonin could occur because the receptor desensitizes rapidly to the bath-applied agonist or the endogenous serotonin can fully activate the receptors involved the initiation of spontaneous synchronous activity.

Because the serotonergic neurones are not the only cells in the midline regions, it remains possible that the non-neuronal ventricular zone cells or non-serotonergic neurones present in our midline regions participate in

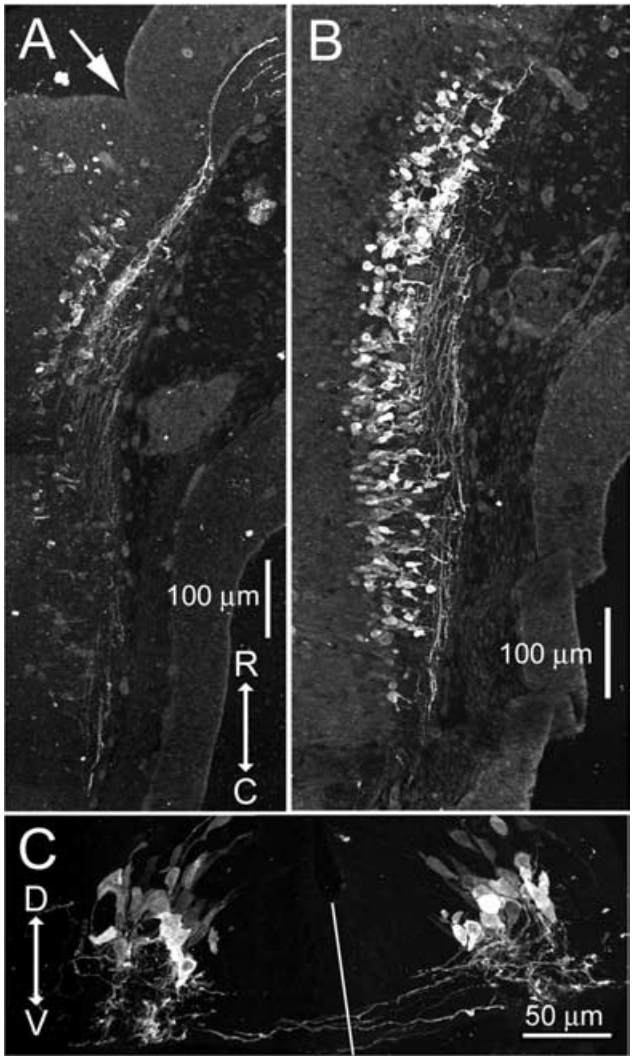

Figure 4. Serotonin is expressed in the hindbrain midline of the E11.5 embryo, shown in immunocytochemical labelling of 20 μm cryostat sections
Arrows in *A* and *C* indicate axes of the animal. *A* and *B*, parasagittal sections showing the developing rostral raphe group. *A* is a section 20 μm lateral to the midline of the animal, and shows the rostral–caudal extent of axonal processes; the arrowhead marks the isthmus (midbrain–hindbrain junction), and serotonergic processes can be seen to extend past the isthmus into the midbrain. *B* is 40 μm more lateral, and shows the group of cell bodies covering approximately 680 μm in the rostral hindbrain; immunopositive somata are not seen outside of the hindbrain. *C* is a horizontal section showing serotonin-immunopositive neurones immediately adjacent to the midline with axons ramifying extensively in the marginal zone, and extending across the midline. Section is positioned with ventricular zone towards the top of the picture.

some way in the activity. To investigate this possibility, we assayed the fraction of total neurones in our defined midline region that the serotonergic cells represent, and determined directly the participation of non-neuronal ventricular zone cells in spontaneous activity.

To determine the fraction of midline neurones that are serotonergic, cryosections were immunoreacted against both serotonin and the neuronal marker TuJ1, and sections were then counterstained with DAPI to show nuclei within the hindbrain slices (Fig. 7). Cells within 125 μm of the midline were then counted, and TuJ1-expressing neurones classified by whether they expressed serotonin. The ventricular zone was identified as a continuous array of relatively elongated nuclei, with no TuJ1 staining. In our sample of sections ($n = 789$ neurones in 11 sampled regions), $82 \pm 7\%$ of all TuJ1-positive neurones within 125 μm of the midline were serotonin-positive. This count includes newly differentiated neurones with ventricular zone processes. Thus, the majority of neurones within the region where spontaneous activity initiates in the hindbrain are serotonergic.

In order to confirm that activity arises in these serotonergic cell bodies, rather than in the overlying (more dorsally located) ventricular zone cells, we performed $[Ca^{2+}]_i$ imaging on horizontal embryo slices, in which these zones can be more easily distinguished ($n = 8$). The fluo-4-loaded cells are shown in Fig. 8*A*, and the ventricular zone can be discriminated from the marginal zone, as it loads poorly with the $[Ca^{2+}]_i$ indicator. Individual recording sites were arrayed across both sides of the tissue slice in the ventricular zone, in the region containing cell somata (future grey matter) and in the marginal zone containing cellular processes and axons. Activity can be observed to initiate at the midline, and propagate laterally in the marginal zone (upper set of traces in Fig. 8*C*) and in the zone of neuronal somata (data not shown). Some events failed to propagate in the more lateral regions. However, no $[Ca^{2+}]_i$ events are observed in any position of the ventricular zone (lower set of traces in Fig. 8*C*), indicating that this region does not initiate or contribute to the spontaneous activity in the hindbrain. Regions on the contralateral side of the hindbrain were also synchronized (shown by a site in the somata-containing zone), although one event did not propagate contralaterally. Similar results were seen in six experiments. The same 200 μm thick tissue section was then processed for immunocytochemistry against serotonin, and is shown overlaid on the fluo-4-generated $[Ca^{2+}]_i$ image in Fig. 8*B*. Although the slice is slightly misshapen because of the thickness and because of the processing for immunocytochemistry, it is clear that serotonin-positive neurones are situated just lateral to the midline ventricular cells.

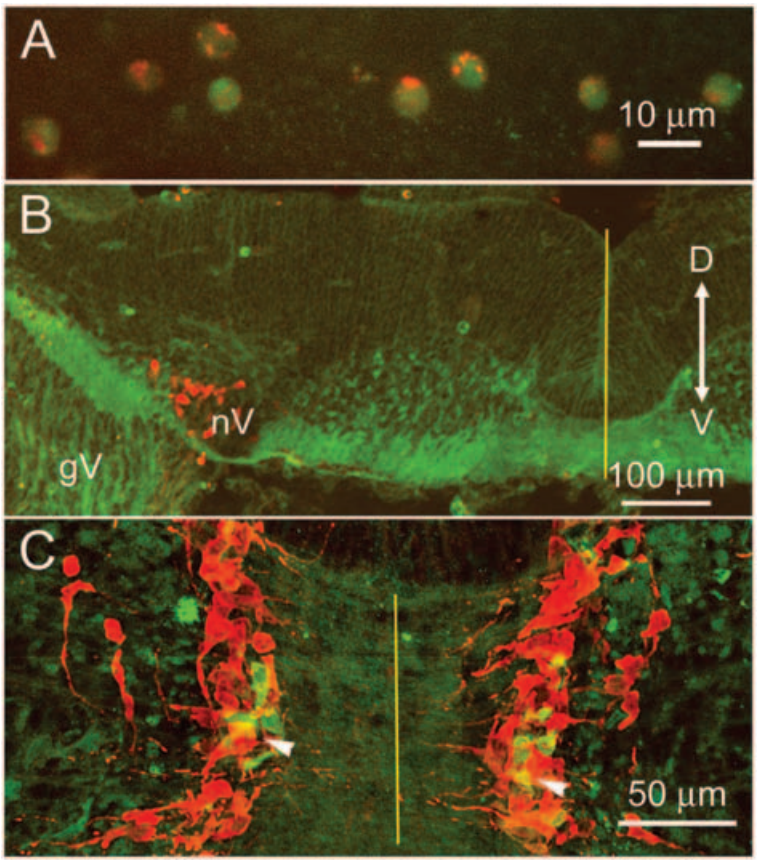

Figure 5. The 5-HT$_{2A}$ receptor is expressed in regions appropriate for mediating propagation of activity
A, fluo-4-loaded dextran-injected motor neurones during $[Ca^{2+}]_i$ imaging experiment. *B*, horizontal 20 μm cryostat section demonstrating immunoreactivity for the 5-HT$_{2A}$ receptor. Strong staining is observed in the midline commissural area (vertical line indicates midline), and in the marginal zone lateral to the midline. This animal was dextran-injected in the b1 branchial arch, and motor neurones can be seen in the V motor group (nV) in red. Strong receptor immunoreactivity is also observed in the sensory axons of the Vth sensory ganglion (gV). Arrows at right of figure show the dorsal and ventral axes, and apply to part *C* as well.
C, co-immunolabelling for serotonin reactivity (red) and 5-HT$_{2A}$ receptor (green). Receptor immunoreactivity is strong in processes crossing the midline, in a few serotonin-immunolabelled neurones immediately lateral to the midline (arrowheads), and in the marginal zone extending laterally. Vertical bar indicates midline.

(The thicker slices also tend to have higher background fluorescence after processing for immunocytochemistry; thus the red signal at the anatomical midline of the section.) This is the region where activity originated in the slice during $[Ca^{2+}]_i$ imaging, and underscores the anatomical correlation between the location of the serotonergic neurones and the specific region in which spontaneous activity originates.

Discussion

The experiments presented above suggest that midline neurones of the developing serotonergic raphe system in the embryonic hindbrain participate in initiating spontaneous, synchronous activity, and in fact may be the primary initiators of this activity that occurs in the hindbrain at E11.5. (1) Although spontaneous activity occurs throughout the entire hindbrain, bilaterally and synchronously, it is initiated within 63 μm on either side of anatomical midline and propagates laterally from there. (2) When lateral regions are surgically isolated from the midline, the frequency of activity in the midline is unaffected whereas activity in lateral regions disappears entirely or is reduced in frequency. (3) A band of serotonin-expressing neuronal somata is located in the 125 μm region of the midline where activity originates, and they represent more than 80% of all neurones in that midline region. Activity does not occur in non-neuronal ventricular zone or floor plate cells, the other major cell types in the midline region. (4) The 5-HT_{2A} receptor was immunolocalized to the region of decussating axons, the serotonergic neurones, and the marginal zone of the entire hindbrain, a position appropriate for mediating the lateral and contralateral propagation of spontaneous activity. (5) Receptor antagonists specific to the 5-HT_{2A} receptor block spontaneous activity, whereas other serotonin receptor subtype antagonists, or glutamate, glycine, GABA, noradrenaline and ACh receptor antagonists, either alone or in combination, do not.

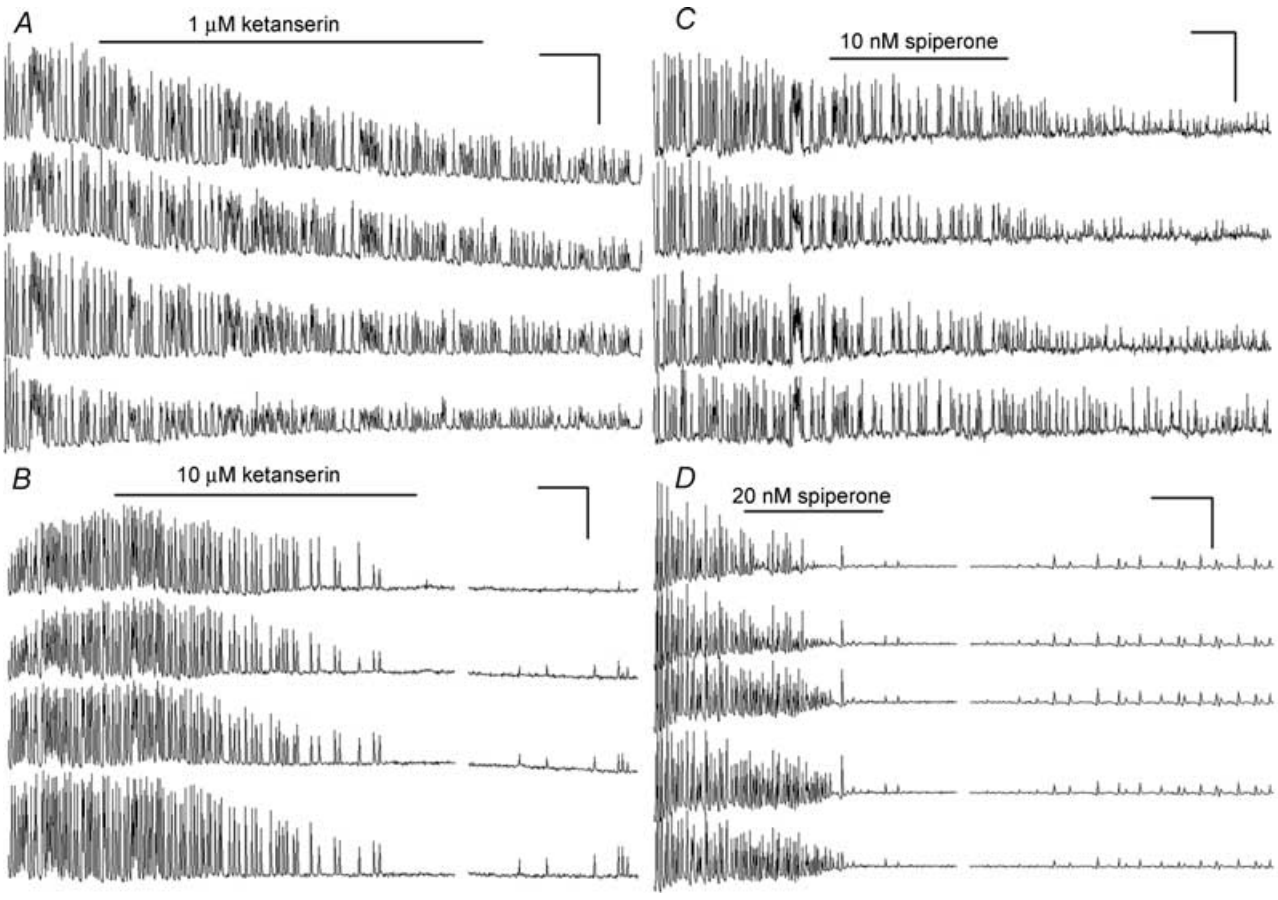

Figure 6. Pharmacological manipulation of spontaneous activity in hindbrain
A, 1 μM ketanserin has little effect on spontaneous activity. *B*, 10 μM ketanserin completely blocks spontaneous activity, which returns upon washout of the drug. Gap in time axis is 40 min. *C*, 10 nM spiperone slightly reduces the frequency of spontaneous activity. *D*, 20 nM spiperone completely blocks spontaneous activity, which returns upon washout of the drug. Gap in time axis is 15 min. Vertical scale bars are 3 units of change in fluorescence for panels *A*, *B* and *D*, 2 units of change in fluorescence for panel *C*; horizontal scale bars are 5 min for all panels.

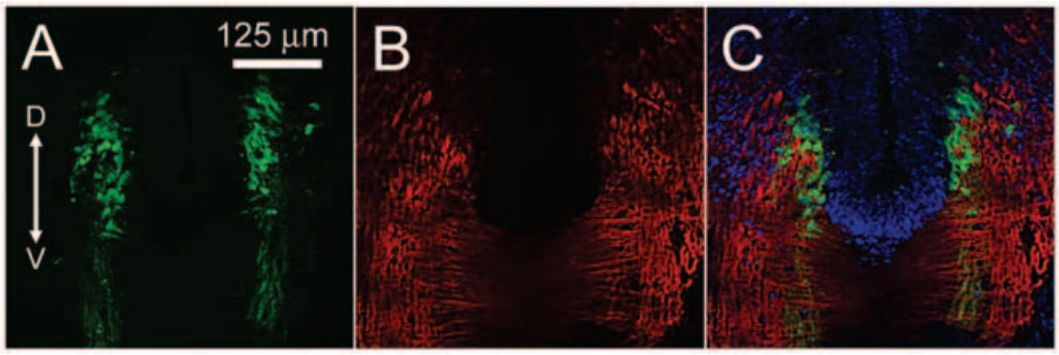

Figure 7. Serotonergic neurones are the majority of neurones in the midline region
The same section is shown labelled for serotonin (*A*, green), TuJ1 (*B*, red), and the merged image (*C*) of serotonin, TuJ1 and DAPI (blue). The scale bar of 125 μm applies to all three images; as do the arrows indicating axes. Both sides of the hindbrain are shown, with the ventricular zone positioned towards the top of the picture.

Regions that initiate or drive activity have not been clearly demonstrated in other areas of the developing brain where synchronized spontaneous activity is observed. In developing chick spinal cord, the higher excitability of motor neurones is postulated to activate Renshaw-like interneurones, which then synchronize activity throughout the spinal cord by enhancing network excitation (Wenner & O'Donovan, 2001). In the developing hippocampus, either septal or hilar neurones have been postulated to drive synchronous activity (Strata *et al.* 1997; Leinekugel, 1998). Neither region, however, appears to be capable of independent activity when isolated.

In the developing rat hippocampus, spontaneous activity takes the form of giant depolarizing potentials (GDPs) or early network oscillations (ENOs), driven

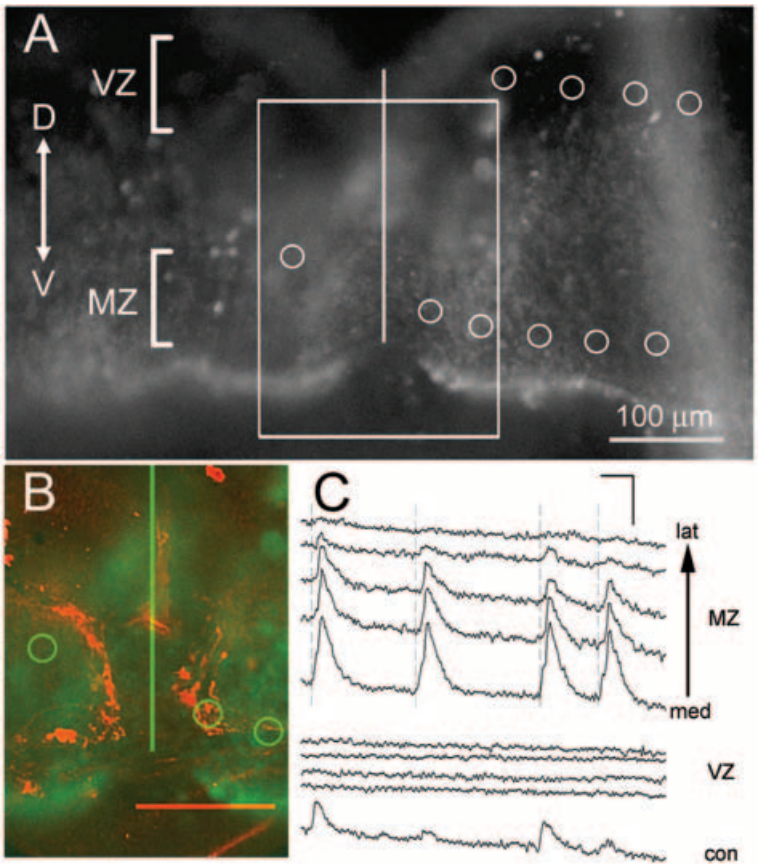

Figure 8. Medial-to-lateral activity is contained within a single 200 μm horizontal slices
A, a horizontal section of a E11.5 embryo loaded with fluo-4 during a $[Ca^{2+}]_i$ imaging experiment. The midline is shown by the vertical line, and the cell-free marginal zone (MZ) and proliferative ventricular zone (VZ) are indicated with brackets. Arrows indicate the dorsal and ventral axes of the tissue. Recording regions span the tissue from the midline to the more lateral regions (open circles) in both the MZ and VZ, and on the contralateral side. Activity recorded from these regions is shown in panel *C*. Boxed region shows the area of the slice that is shown in part *B*. *B*, central region of the fluo-4-loaded slice from *A* (green), overlaid with the images from the same slice after one hour fixation with 4% PFA and immunocytochemistry for serotonin (red). Neurones with extensive processes are seen on both sides of the midline (vertical line). Scale bar is 100 μm, the same as part *A*. *C*, records of activity from recording areas in the marginal zone (MZ), the ventricular zone (VZ) or the contralateral side (con). Scale bars are 3 units of fluorescence change and 10 s. Arrow indicates medial to lateral position of recording sites both in the marginal zone and ventricular zone traces.

primarily by GABA excitation during the stages when the Cl^- equilibrium potential is relatively positive (Ben-Ari *et al.* 1989; Garaschuk *et al.* 1998; Ben-Ari, 2002). Widespread synchronous activity in the developing cortex has been shown by $[Ca^{2+}]_i$ imaging (Garaschuk *et al.* 2000; Corlew *et al.* 2004). This activity is not blocked by antagonists of the $GABA_A$ receptor although GABA is excitatory, but is sensitive to pharmacological blockade of both NMDA and non-NMDA receptors (Leinekugel *et al.* 1997). In contrast to neonatal cortical slices, neonatal cortical neurones in dispersed cultures generate synchronous activity that appears to emanate from a population of GABAergic subplate neurones (Voigt *et al.* 2001). Spontaneous activity in the chick spinal cord is driven by redundant glutamatergic, nicotinic and GABAergic/glycinergic systems, acting in a network system of mutual excitation to drive synchronicity (Chub & O'Donovan, 1998; O'Donovan, 1999; Tabak *et al.* 2001). Although the network changes the dependence on these transmitters over developmental time, they may substitute for each other under experimental conditions. In mouse spinal cord, motor neurones acting via nicotinic receptors and GABAergic interneurones can generate local episodes of spontaneous activity, while the ability to spread that activity between segments requires glycinergic components (Hanson & Landmesser, 2003). The serotonergic dependence of spontaneous activity in these developing brain regions has not been tested. The hindbrain may be unique in utilizing serotonin to initiate and propagate spontaneous activity, perhaps due to the fact that the raphe system is developing within it. A dependence on serotonin of the late fetal respiratory rhythm has been demonstrated in rats (Di Pasquale *et al.* 1994).

We have shown that spontaneous synchronized activity initiates in a relatively narrow region around the rostral midline of the hindbrain, in the exact position where a large population of serotonergic neurones are differentiating. We have demonstrated that over 80% of the neurones at the midline are serotonergic; the identity of the remaining neurones is not known. In order to ascertain whether the fluo-4-loaded midline neurones that are in the region of activity initiation are serotonergic, we attempted to immunolabel the fluo-4-loaded neurones using the fixative 1-ethyl-3-(3-dimethylaminopropyl)carbodiimide (EDC), which has been shown to fix calcium indicators and chelators in cells (Tymianski *et al.* 1997). However, whether we used 3% EDC in ACSF ($n = 7$), or a combination of 4% PFA–1% EDC in ACSF ($n = 3$) or 4% PFA–3% EDC in ACSF ($n = 2$), the fluo-4 signal was not observed, and the immunoreactivity for serotonin was degraded. These experiments do not clarify whether the active, fluo-4-loaded neurones were actually the serotonergic neurones that initiate activity. However, the overlay of the fluo-4-loaded neurones with the serotonin immunoreactivity in the same slice, shown in Fig. 8*B*, demonstrates that the region where activity initiates in these $[Ca^{2+}]_i$ imaging experiments is indeed serotonergic. It is possible that serotonin released tonically from midline neurones is acting in a permissive manner to allow other midline neuronal cells to generate activity; however, given that less than 20% of the midline neurones are not serotonergic-immunopositive and that non-neuronal cells are not active, this is an unlikely scenario. Thus, whether serotonergic neurones are acting as independently active pacemakers or in a mutually excitatory network that includes a relatively small proportion of other neurones, it is highly probable that they are the major initiators of the activity that is then propagated through the hindbrain.

It is possible that a proportion of midline neurones are serotonin-immunopositive due to the uptake of surrounding transmitter rather than by biosynthesis. This is unlikely, since in rat, the expression of the ETS domain transcription factor PET-1, a specific marker for serotonergic neurones, is restricted to neurones that coexpress the synthetic enzymes for serotonin and the serotonin transporter (Hendricks *et al.* 1999); thus the neurones expressing the transporter are themselves serotonergic. In mouse, the serotonin transporter is expressed in rostral hindbrain very closely opposed to the midline (Bruning *et al.* 1997). Even if some proportion of neurones do not synthesize serotonin, they are probably involved in signalling by serotonin, and are likely to play a role in the generation of spontaneous activity.

Spontaneous activity in the developing cortex has been shown to be initiated and propagated in the ventricular zone by radial glial cells (Weissman *et al.* 2004). We demonstrate here that the activity that we observe is neither generated nor propagated in the ventricular zone of the hindbrain. Radial glial cells, identified by RC2 immunoreactivity, are relatively sparse in the hindbrain at this point of development (data not shown), and we have not observed propagation of a signal from the ventricular zone towards the pial surface or *vice versa* in slice experiments. The serotonergic neurones are the most medial differentiated group of neurones in the hindbrain. Medially positioned branchiomeric motor neurones differentiate relatively early, but migrate laterally, while non-branchiomeric motor neurones (cranial nerves IV and VI) are not found at the same rostro-caudal position in the hindbrain as the serotonergic neurones at E11.5.

Because some of the isolated lateral regions of the hindbrain are able to maintain a slow rhythm in the presumed absence of midline serotonergic inputs, it is possible that hindbrain neuronal populations participate in excitatory network interactions that prime the tissue for spontaneous activity. Our experiments suggest that the midline serotonergic neurones provide the additional excitatory inputs that then initiate widespread activity.

Application of the serotonergic agonist DOI did not consistently activate or increase activity in isolated lateral regions: in one experiment, DOI (50 μM) caused one transient in quiescent lateral tissue; an average increase in frequency of 1.66 (to an average rate of 1.45 events min^{-1}, $n = 2$, 20 μM DOI) in two experiments; and no effect in another (20 μM). However, these frequencies are not similar to those of midline regions or of lateral regions before the surgical separation. These experiments may be difficult to interpret, since the network properties of the cut tissue may be modified by the surgery.

The serotonergic system is broadly distributed throughout the central nervous system, and numerous behaviour disorders are attributed to serotonin deficiencies that may be associated with developmental abnormalities (Whitaker-Azmitia, 2001). Excess serotonin is implicated in autism-related disease, whereas deficits in serotonin predispose to mood disorders (Chugani *et al.* 1999; Betancur *et al.* 2002; Gross *et al.* 2002). The serotonergic system is also implicated in development of the cortex (Luo *et al.* 2003; Vitalis & Parnavelas, 2003), and neuronal differentiation (Lauder *et al.* 2000). In addition, neurones of the dorsal raphe, which innervate the frontal cortex widely, are rhythmically active during waking states, indicating a role for these neurones in general arousal of the CNS (Jacobs & Fornal, 1991). Spontaneous activity may be a feature of serotonergic neurones at all points in their maturation: this activity may be important in formation of physiological circuits within the developing CNS as well as having an important neuromodulatory function in the adult CNS.

References

Barnes NM & Sharp T (1999). A review of central 5-HT receptors and their function. *Neuropharmacology* **38**, 1083–1152.

Ben-Ari Y (2002). Excitatory actions of GABA during development: the nature of the nurture. *Nature Rev Neurosci* **3**, 728–739.

Ben-Ari Y, Cherubini E, Corradetti R & Gaiarsa JL (1989). Giant synaptic potentials in immature rat CA3 hippocampall neurones. *J Physiol* **416**, 303–325.

Betancur C, Corbex M, Spielewoy C, Philippe A, Laplanch JL, Launay JM, Gillberg C, Mouren-Simeoni MC, Hamon M, Giros B, Nosten-Bertrand M & Leboyer M (2002). Serotonin transporter gene polymorphisms and hyperserotonemia in autistic disorder. *Mol Psychiatry* **7**, 67–71.

Bruning G, Liangos O & Baumgarten HG (1997). Prenatal development of the serotonin transporter in mouse brain. *Cell Tissue Res* **289**, 211–221.

Chub N & O'Donovan MJ (1998). Blockade and recovery of spontaneous rhythmic activity after application of neurotransmitter antagonists to spinal networks of the chick embryo. *J Neurosci* **18**, 294–306.

Chugani DC, Muzik O, Behen M, Rothermal R, Janisse JJ, Lee J & Chugani HT (1999). Developmental changes in brain serotonin synthesis capacity in autistic and nonautistic children. *Ann Neurol* **45**, 287–295.

Corlew R, Bosma MM & Moody WJ (2004). Spontaneous, synchronous electrical activity in neonatal mouse cortical neurones. *J Physiol* **560**, 377–390.

Di Pasquale E, Monteau R & Hilaire G (1994). Endogenous serotonin modulates the fetal respiratory rhythm: an in vitro study in the rat. *Brain Res Dev Brain Res* **80**, 222–232.

Feller MB (1999). Spontaneous correlated activity in developing neural circuits. *Neuron* **22**, 653–656.

Fortin G, Kato F, Lumsden A & Champagnat J (1995). Rhythm generation in the segmented hindbrain of chick embryos. *J Physiol* **486**, 735–744.

Garaschuk O, Hanse E & Konnerth A (1998). Developmental profile and synaptic origin of early network oscillations in the CA1 region of rat neonatal hippocampus. *J Physiol* **507**, 219–236.

Garaschuk O, Linn J, Eilers J & Konnerth A (2000). Large-scale oscillatory calcium waves in the immature cortex. *Nature Neurosci* **3**, 452–459.

Gross C, Zhuang X, Stark K, Ramboz S, Oosting R, Kirby L, Santarelli L, Beck S & Hen R (2002). Serotonin1A receptor acts during development to establish normal anxiety-like behaviour in the adult. *Nature* **416**, 396–400.

Gust J, Wright JJ, Pratt EB & Bosma MM (2003). Development of synchronized activity of cranial motor neurons in the segmented embryonic mouse hindbrain. *J Physiol* **550**, 123–133.

Hanson MG & Landmesser LT (2003). Characterization of the circuits that generate spontaneous episodes of activity in the early embryonic mouse spinal cord. *J Neurosci* **23**, 587–600.

Hendricks T, Francis N, Fyodorov D & Deneris ES (1999). The ETS domain factor Pet-1 is an early and precise marker of central serotonin neurons and interacts with a conserved element in serotonergic genes. *J Neurosci* **19**, 10348–10356.

Hendricks TJ, Fyodorov DV, Wegman LJ, Lelutiu NB, Pehek EA, Yamamoto B, Silver J, Weeber EJ, Sweatt JD & Deneris ES (2003). Pet-1 ETS gene plays a critical role in 5-HT neuron development and is required for normal anxiety-like and aggressive behavior. *Neuron* **37**, 233–247.

Jacobs BL & Fornal CA (1991). Activity of brain serotonergic neurons in the behaving animal. *Pharmacol Rev* **43**, 563–578.

Lauder JM, Wilkie MB, Wu C & Singh S (2000). Expression of 5-HT$_{2A}$, 5-HT$_{2B}$ and 5-HT$_{2C}$ receptors in the mouse embryo. *Int J Dev Neurosci* **18**, 653–662.

Leinekugel X, Khalilov I, Ben-Ari Y & Khazipov R (1998). Giant depolarizing potentials: the septal pole of the hippocampus paces the activity of the developing intact septohippocampal complex *in vitro*. *J Neurosci* **18**, 6349–6357.

Leinekugel X, Medina I, Khalilov I, Ben-Ari Y & Khazipov R (1997). Ca^{2+} oscillations mediated by the synergistic excitatory actions of GABA$_A$ and NMDA receptors in the neonatal hippocampus. *Neuron* **18**, 243–255.

Luo X, Persico AM & Lauder JM (2003). Serotonergic regulation of somatosensory cortical development: lessons from genetic mouse models. *Dev Neurosci* **2**, 173–183.

Menendez de la Prida L & Sanchez-Andres JV (2000). Heterogeneous populations of cells mediate spontaneous synchronous bursting in the developing hippocampus through a frequency-dependent mechanism. *Neuroscience* **97**, 227–241.

Moody WJ & Bosma MM (2005). Ion channel development, spontaneous activity, and activity-dependent development in nerve and muscle cells. *Physiol Rev* (in press).

O'Donovan MJ (1999). The origin of spontaneous activity in developing networks of the vertebrate nervous system. *Curr Opin Neurobiol* **9**, 94–104.

Strata F, Atzori M, Molnar M, Ugolini G, Tempia F & Cherubini E (1997). A pacemaker current in dye-coupled hilar interneurons contributes to the generation of giant GABAergic potentials in developing hippocampus. *J Neurosci* **17**, 1435–1446.

Tabak J, Rinzel J & O'Donovan MJ (2001). The role of activity-dependent network depression in the expression and self-regulation of spontaneous activity in the developing spinal cord. *J Neurosci* **21**, 8966–8978.

Tymianski M, Bernstein GM, Abdel-Hamid KM, Sattler R, Velumian A, Carlen PL, Razavi H & Jones OT (1997). A novel use for a carbodiimide compound for the fixation of fluorescent and non-fluorescent calcium indicators in situ following physiological experiments. *Cell Calcium* **21**, 175–183.

Vitalis T & Parnavelas JG (2003). The role of serotonin in early cortical development. *Dev Neurosci* **25**, 245–256.

Voigt T, Opitz T & de Lima AD (2001). Synchronouse oscillatory activity in immature cortical network is driven by GABAergic preplate neurons. *J Neurosci* **21**, 8895–8905.

Weissman TA, Riquelme PA, Ivic L, Flint AC & Kriegstein AR (2004). Calcium waves propagate through radial glial cells and modulate proliferation in the developing neocortex. *Neuron* **43**, 647–661.

Wenner P & O'Donovan MJ (2001). Mechanisms that initiate spontaneous network activity in the developing chick spinal cord. *J Neurophysiol* **86**, 1481–1498.

Whitaker-Azmitia PM (2001). Serotonin and brain development: Role in human developmental diseases. *Brain Res Bull* **56**, 479–485.

Acknowledgements

Funded by NSF ADVANCE SBE-0123552; IBN 031 5831. We appreciate numerous discussions with Drs W. Moody and J. Truman, and thank Drs W. Moody and B. Hille for reading earlier versions of the manuscript and J. Gust for early experimental input.